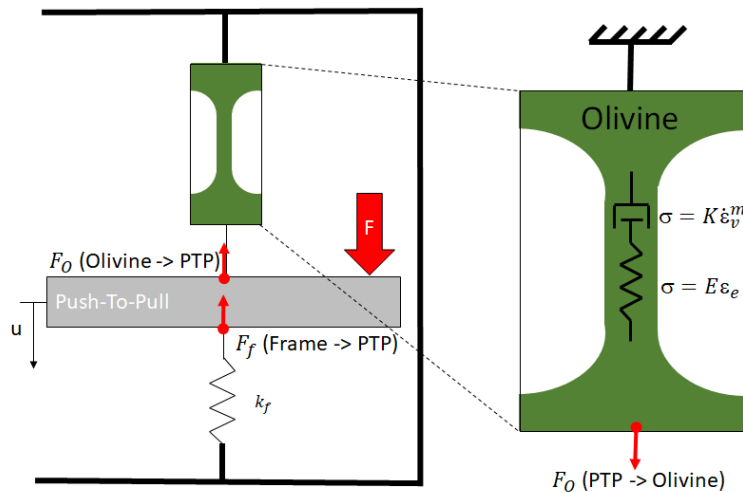


## Mechanical model of the Push-to-Pull device<sup>1</sup>

Baral *et al.* (2021) have shown from nanoindentation relaxation experiments that  $\alpha$ -olivine exhibits some creep at room temperature with a constant strain rate sensitivity up to 0.052, over seven orders of magnitude in strain-rate. An increase of about 0.8 GPa is expected when the strain rate is 1000 times higher. This constant strain rate sensitivity has already been observed in silica glass but with a significantly lower magnitude than the one of  $\alpha$ -olivine (Storm *et al.* 2005). Therefore, it may be assumed that plastic flow of such glasses is mostly thermally-activated and can be modelled through a simple elastic-viscoplastic formalism without a time-independent yield threshold.



**Figure S6.** 1D model used to extract the viscoplastic behavior of materials deformed with the PTP setup.

In the model proposed here (Figure S6), elasticity of  $\alpha$ -olivine is considered as linear and isotropic ( $\sigma = E \varepsilon_e$ ) with a Young modulus of 41 GPa as measured on sample OL-4. A power-law creep ( $\sigma = K \dot{\varepsilon}_v^m$ ) is chosen to describe the viscoplastic flow where  $K = 4.7 \text{ GPa}\cdot\text{s}^{-m}$  and  $m = 0.052$  as measured from nanoindentation relaxation tests (Baral *et al.* 2021). It is important to keep in

<sup>1</sup> From A. Orekhov, G. Kermouche, A. Gomez-Perez, P. Baral, R. Dohmen, M. Coulombier, J. Verbeeck, T. Pardoën, D. Schryvers, J. Lin, P. Cordier & H. Idrissi (2024) Room temperature electron beam sensitive viscoplastic response of ultra-ductile amorphous olivine films. *Acta Materialia*, 282, 120479. <https://doi.org/10.1016/j.actamat.2024.120479>

mind that the stiffness of the PTP device acts as a spring connected in parallel to the tensile sample (Figure S6). Therefore, the applied load is split into a force  $F_O$  acting on the sample and a force  $F_f$  acting on the device frame:

$$F = F_O(\text{olivine} \rightarrow \text{PTP}) + F_f(\text{Frame} \rightarrow \text{PTP}) \quad (\text{Eq. S1})$$

The strain-rate and stress are computed respectively as  $\dot{\epsilon} = \frac{\dot{u}}{L}$  and  $\sigma = \frac{F_O}{S}$ , where  $\dot{u}$  is the displacement rate,  $L$  is the sample length and  $S$  is the sample section. The strain rate  $\dot{\epsilon}$  can be split into an elastic part  $\dot{\epsilon}_e$  and a viscoplastic part  $\dot{\epsilon}_v$ . Rearranging these equations, it comes:

$$\dot{F}_O = \left( \frac{Lk_f}{Lk_f + ES} \right) \left( \frac{ES}{Lk_f} \dot{F} + \sigma \dot{S} - ES \left( \frac{\sigma}{K} \right)^{\frac{1}{m}} \right) \quad (\text{Eq. S2})$$

From this equation, it appears that the maximum stress reached during the test, roughly determined through  $\dot{F}_O = 0$ , depends upon a-olivine rheological parameters, the loading rate  $\dot{F}$  but also on the frame stiffness  $k_f$ . It is thus worth noting that yield stress of time-dependent materials measured from PTP-based tensile testing depends on frame stiffness.

From Eq. S2, the stress rate can be negative upon loading if the viscoplastic strain rate  $\dot{\epsilon}_v = \left( \frac{\sigma}{K} \right)^{\frac{1}{m}}$  increases drastically, which is likely to occur when switching on the electron beam. Eq. S2 also points out the key role of the frame stiffness over such a behavior (see Figure S7). Our model could thus be used as a tool for running an inverse identification procedure aiming at determining the rheological parameters of a-olivine under beam-on conditions. Such a methodology would however require to run several experimental tests under various conditions to avoid any effects of experimental uncertainties on the results. Here we propose to restrain our analysis to the direct measurement of the strain rate sensitivity during the beam-on induced stress relaxation of a-olivine. Indeed, according to this simple 1D model the strain rate sensitivity can be defined as follow:

$$m = \frac{d \text{Log}(\sigma)}{d \text{Log}(\dot{\epsilon}_v)} \quad (\text{Eq. S3})$$

where the (visco)plastic strain-rate  $\dot{\epsilon}_v$  can be computed as  $\dot{\epsilon}_v = \dot{\epsilon} - \frac{\dot{\sigma}}{E}$ .

For each experiment, the Young modulus has been set to the one given in Table 3, and remains the same both for beam off and beam on conditions. This is consistent with the tensile tests results of Fig. 4a, which do not point any effect of the beam on the elastic modulus. Eventually the only fitting parameter is the PTP stiffness  $k_f$ . The regression analysis is conducted using a classical minimization of the sum of squared residuals between experimental and numerical stress strain curves.

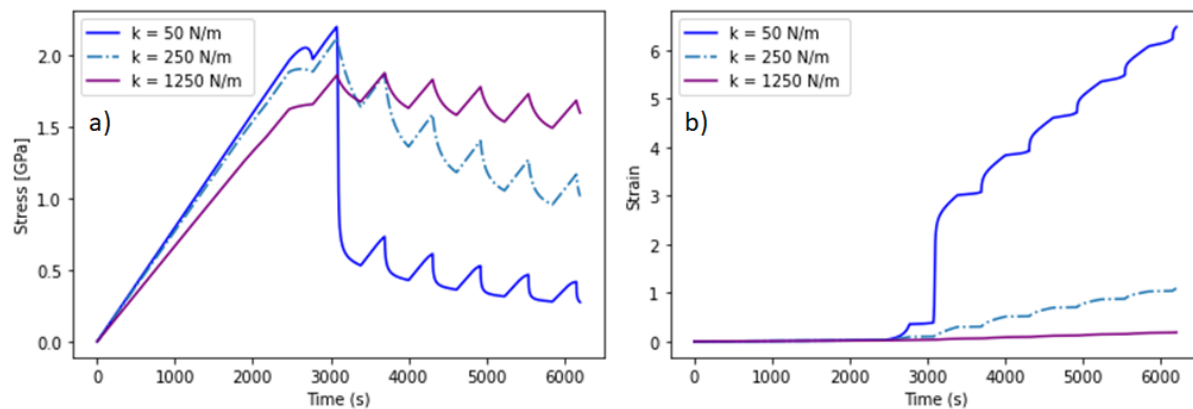


**Figure S7.** 1D simulation of alternating beam-on and beam-off conditions with increasing values of the frame stiffness. a) stress versus time and b) strain versus time. Eq. S3 points out the key role of the frame stiffness in the viscoelastic behavior. To highlight this effect, the 1D model presented in Fig. 7 has been run using different values of the frame stiffness. The “beam-on” a-olivine has the same elastic viscoplastic properties than the “beam off” a-olivine but with a sensitivity to strain rate that is increased by a factor of two. The results are plotted in this figure. The stress relaxation and the strain rate increase during the beam-on mode are well reproduced. The frame stiffness plays a role on the magnitude of the stress relaxation as well as on the strain rate level. To some extent, changing the frame stiffness allows for investigating various strain rate domains without changing the loading rate.